

# Osteoarthritis and Cartilage



## Characterization of rhodanine derivatives as potential disease-modifying drugs for experimental mouse osteoarthritis

J.-S. Kwak <sup>† a</sup>, Y. Lee <sup>† a</sup>, J. Yang <sup>†</sup>, S.K. Kim <sup>†</sup>, Y. Shin <sup>†</sup>, H.-J. Kim <sup>†</sup>, J.H. Choi <sup>†</sup>, Y.J. Im <sup>†</sup>, M.-J. Kim <sup>§</sup>, K. Lee Yu <sup>||</sup>, J. Chang You <sup>§ ||</sup>, J.-S. Chun <sup>†\*</sup>

<sup>†</sup> National Creative Research Initiatives Center for Osteoarthritis Pathogenesis and School of Life Sciences, Gwangju Institute of Science and Technology, Gwangju, 61005, Republic of Korea

<sup>‡</sup> College of Pharmacy, Chonnam National University, Gwangju, 61186, Republic of Korea

<sup>§</sup> Avixgen Inc., Seoul, 06649, Republic of Korea

<sup>||</sup> National Research Laboratory for Molecular Virology, Department of Pathology, School of Medicine, The Catholic University of Korea, Seoul, 06591, Republic of Korea

### ARTICLE INFO

#### Article history:

Received 8 July 2021

Accepted 26 April 2022

#### Keywords:

Osteoarthritis

Posttraumatic OA

Mouse

Chondrocytes

Rhodanine-derived compounds

Disease-modifying OA drug (DMOAD)

Therapeutics

### SUMMARY

**Objective:** This study was performed to characterize selected rhodanine derivatives as potential preclinical disease-modifying drugs for experimental osteoarthritis (OA) in mice.

**Methods:** Three rhodanine derivatives, designated rhodanine (R)-501, R-502, and R-503, were selected as candidate OA disease-modifying drugs. Their effects were evaluated by intra-articular (IA) injection in OA mouse models induced by DMM (destabilization of the medial meniscus) or adenoviral overexpression in joint tissues of hypoxia-inducible factor (HIF)-2 $\alpha$  or zinc importer ZIP8. The regulatory mechanisms impacted by the rhodanine derivatives were examined in primary-culture chondrocytes and fibroblast-like synoviocytes (FLS).

**Results:** All three rhodanine derivatives inhibited OA development caused by DMM or overexpression of HIF-2 $\alpha$  or ZIP8. Compared to vehicle-treated group, for example, IA injection of R-501 in DMM-operated mice reduced median OARSIS grade from 3.78 (IQR 3.00–5.00) to 1.89 (IQR 0.94–2.00,  $P = 0.0001$ ). R-502 and R-503 also reduced from 3.67 (IQR 2.11–4.56) to 2.00 (IQR 1.00–2.00,  $P = 0.0030$ ) and 2.00 (IQR 1.83–2.67,  $P = 0.0378$ ), respectively. Mechanistically, the rhodanine derivatives inhibited the nuclear localization and transcriptional activity of HIF-2 $\alpha$  in chondrocytes and FLS. They did not bind to Zn<sup>2+</sup> or modulate Zn<sup>2+</sup> homeostasis in chondrocytes or FLS; instead, they inhibited the nuclear localization and transcriptional activity of the Zn<sup>2+</sup>-dependent transcription factor, MTF1. HIF-2 $\alpha$ , ZIP8, and interleukin-1 $\beta$  could upregulate matrix-degrading enzymes in chondrocytes and FLS, and the rhodanine derivatives inhibited these effects.

**Conclusion:** IA administration of rhodanine derivatives significantly reduced OA pathogenesis in various mouse models, demonstrating that these derivatives have disease-modifying therapeutic potential against OA pathogenesis.

© 2022 Published by Elsevier Ltd on behalf of Osteoarthritis Research Society International.

### Introduction

Osteoarthritis (OA) can be initiated by multiple etiological risk factors, including mechanical stress, metabolic stress, and/or inflammation<sup>1–3</sup>. These risk factors cause whole-joint disorders,

such as cartilage destruction, synovial inflammation, osteophyte formation, and subchondral bone sclerosis<sup>4</sup>. Progressive degeneration of articular cartilage is a hallmark of OA. Therefore, chondrocytes are acknowledged to play a central role in OA pathogenesis<sup>4</sup>. An imbalance between anabolic and catabolic factors in chondrocytes, such as matrix-degrading enzymes and/or cartilage extracellular matrix (ECM) molecules, plays an important role in the dysregulation of cartilage matrix homeostasis in OA<sup>5,6</sup>. Animal model-based studies revealed that matrix metalloproteinase (MMP)3, MMP13, and ADAMTS5 play crucial roles in OA cartilage destruction<sup>7–9</sup>.

\* Address correspondence and reprint requests to: J.-S. Chun, School of Life Sciences, Gwangju Institute of Science and Technology, Gwangju 61005, Republic of Korea. Tel: 82-62-715-2497; Fax: 82-62-715-2484.

E-mail address: jschun@gist.ac.kr (J.-S. Chun).

<sup>a</sup> These authors contributed equally to this work.

Among the various experimental OA models in mice, destabilization of the medial meniscus (DMM) is the best characterized post-traumatic OA model that exhibits most of the manifestations of OA<sup>10</sup>. We previously identified several critical catabolic mediators of OA pathogenesis in chondrocytes, including the transcription factor, hypoxia-inducible factor (HIF)-2 $\alpha$ <sup>11,12</sup>, and the zinc importer, ZIP8<sup>13,14</sup>. Our previous results revealed that adenoviral overexpression of HIF-2 $\alpha$  or ZIP8 in joint tissues is sufficient to cause OA development by upregulating matrix-degrading enzymes, even in the absence of mechanical stress, metabolic stress, and/or inflammaging<sup>11–14</sup>. Therefore, the adenoviral overexpression of HIF-2 $\alpha$  and ZIP8 in joint tissues represents two distinct experimental OA models in mice.

Although OA pathogenesis has been extensively studied, no effective disease-modifying therapy for OA has been developed to date. Therefore, it is important to identify and characterize potential disease-modifying drugs for OA. Rhodanine (2-thiothiazolidin-4-one) is a 4-thiazolidinone subtype that exhibits broad and potent activity and has been established as a biologically important scaffold<sup>15</sup>. We previously identified a rhodanine derivative, designated rhodanine-501 (R-501) in this study, that exhibits inhibitory effects on human immunodeficiency virus (HIV) by modulating nucleocapsid protein<sup>16,17</sup>. In other work, rhodanine derivatives have been developed as inhibitors of matrix metalloproteinases (MMPs)<sup>18</sup> and were reported to exhibit *in vitro* anti-degenerative effects on chondrocytes<sup>19</sup>. Here, we examined the possible therapeutic potential of R-501 and two additional structurally related rhodanine derivatives, R-502 and R-503, in various experimental mouse models of OA, including those induced by DMM surgery and adenoviral overexpression of HIF-2 $\alpha$  or ZIP8 in joint tissues. We report here the disease-modifying therapeutic potential of these rhodanine derivatives against experimental OA in mice.

## Materials and methods

### Rhodanine derivatives

We tested three rhodanine derivatives as possible therapeutic drugs for OA. We first examined the therapeutic effects of R-501 and then extended our analysis to R-502 and R-503. The chemical structures of these rhodanine derivatives are presented in [Supplementary Fig. 1\(A\)](#). The methods for synthesizing these compounds were previously described<sup>16</sup>. The purity of the rhodanine derivatives was determined with the Shimadzu LC system (Kyoto, Japan). Sample solution (10  $\mu$ L) was injected on an ODS-C18 column (150  $\times$  4.6 mm, 5  $\mu$ m). Components were resolved in a mixture of water, acetonitrile, and formic acid (35:65:0.05). The flow rate was 1.0 mL/min, and the eluent was detected at 450 nm. The purity of the obtained rhodanine derivatives was >99%. A high-performance liquid chromatogram for R-501 is presented in [Supplementary Fig. 1\(B\)](#).

### Experimental OA in mice

Post-traumatic experimental OA was induced in 12-week-old male C57BL/6J mice by DMM on the right knee<sup>10,13,20</sup>. Sham operation of the left knee of the same mouse was used as a control. Two weeks after operations, mice were injected intra-articularly (IA) with the indicated rhodanine derivatives in a volume of 10  $\mu$ L, once weekly for 3 weeks. We employed IA injection of rhodanine derivatives because our aim was to examine local and direct effects through which the derivatives could have therapeutic potential in joint tissues. Mice were sacrificed at 8 weeks after DMM surgery and subjected to histological analyses. Experimental OA was also

induced by IA injection once weekly for 3 weeks with the indicated plaque forming units (PFUs) of adenovirus expressing HIF-2 $\alpha$  (Ad-HIF-2 $\alpha$ )<sup>11,12</sup> or ZIP8 (Ad-ZIP8)<sup>13,14</sup>. Empty adenovirus (Ad-C) was used as a negative control. Adenovirus was IA injected into both knees of mice. The indicated concentrations of rhodanine derivatives were co-injected with the adenovirus in a total volume of 10  $\mu$ L. Mice were sacrificed at either 3 or 8 weeks after the first IA injection and subjected to histological analyses. The sample size was determined according to the methods established by Arifin *et al.*<sup>21</sup>. We used at least six mice per group to enable comparisons to be made between pairs of groups in multiple-group experiments. The experimental design and numbers of mice in each group are presented in [Supplementary Fig. 2](#). All animal experiments were approved by the Gwangju Institute of Science and Technology Animal Care and Use Committee. All adenoviruses were purchased from Vector Biolabs (Malvern, PA).

### Histology and immunohistochemistry

Knee joint samples were fixed with 4% paraformaldehyde, decalcified in 0.5 M EDTA, embedded in paraffin, sectioned at 5- $\mu$ m thickness, and stained with safranin-O and hematoxylin<sup>13,20</sup>. The modified Mankin's score, OARSI grade, synovitis, and osteophyte formation were calculated as the average scores obtained from three different sections selected at ~100- $\mu$ m intervals. Each section was scored by four observers, and the results are presented as the average value obtained. OARSI grade was expressed as the maximum score observed among the medial femoral condyle, medial tibial plateau, lateral femoral condyle, and lateral tibial plateau<sup>22</sup>. Cartilage ECM loss, which was determined by safranin-O staining, was quantified by modified Mankin's score (score 0: normal, 1: slight reduction, 2: moderate reduction, 3: severe reduction, 4: absent)<sup>23</sup>. Synovitis was determined by scoring synovial inflammation (grade 0–3) in joint sections<sup>24</sup>. Osteophyte formation was identified by safranin-O staining and osteophyte maturity was scored as described previously<sup>13,20</sup>. Subchondral bone sclerosis was indirectly examined by measuring the thickness of the subchondral bone plate (SBP) using an Aperio ImageScope (Vista, CA)<sup>13,20</sup>. The results are presented as average values obtained from three joint sections.

### Primary culture of chondrocytes and fibroblast-like synoviocytes (FLS)

Chondrocytes were isolated from the femoral condyles and tibial plateaus of both knees of 5-day-old ICR mice<sup>25</sup>. Pooled chondrocytes (~10<sup>7</sup> cells) from ~10 pups of littermate were used for one independent experiment. Cells were maintained in Dulbecco's Modified Eagle's Medium (DMEM) supplemented with 10% fetal bovine serum. On culture day 3, cells were treated with interleukin (IL)-1 $\beta$  for 24 h or infected with the indicated multiplicity of infection (MOI) of adenoviruses for 2 h. The cells were maintained for an additional 24 h prior to further analysis. Synovial cells were isolated from both knees of 8-week-old C57BL/6J mice<sup>13,20</sup>. A pool of synovial cells from five mice was passage cultured in DMEM supplemented with 10% fetal bovine serum. Passage 6–8 cells were used as indicated in each experiment. Pure fibroblast-like synoviocytes (FLS) (>90% CD90<sup>+</sup>/ $<$  1% CD14<sup>+</sup>) were identified by flow cytometry using antibodies against CD90 and CD14 (Abcam, Cambridge, UK). The numbers in cell culture experiments indicate independent preparation of chondrocytes or FLS.

### Intracellular Zn<sup>2+</sup> imaging and quantitation

Intracellular Zn<sup>2+</sup> was detected using FluoZin-3 AM (Invitrogen, Waltham, MA)<sup>13,14</sup>, in chondrocytes or FLS. The cells were treated

with IL-1 $\beta$  or infected with Ad-C or Ad-ZIP8, along with the indicated concentrations of rhodanine derivatives. The zinc chelator, TPEN (N,N,N',N'-tetrakis (2-pyridinylmethyl)-1,2-ethanediamine), was used as a positive control. The cells were treated with 1  $\mu$ M of FluoZin-3 AM in the presence of 0.02% Pluronic F-127 (Invitrogen) for 30 min at 37°C, washed with phosphate-buffered saline, and incubated for an additional 30 min at 37°C. Intracellular Zn<sup>2+</sup> images were acquired with a fluorescence microscope, and population-wide fluorescence intensity was measured using a SpectraMax Gemini microplate fluorescence reader (Molecular Devices, San Jose, CA) with excitation set at 488 nm, cut-off at 515 nm, and emission at 530 nm<sup>13,14</sup>. Values for relative Zn<sup>2+</sup> concentration represent the relative fluorescence intensity normalized to the vehicle-treated control group.

#### Immunofluorescence microscopy

Chondrocytes or FLS were treated with IL-1 $\beta$  or infected with Ad-C, Ad-HIF-2 $\alpha$ , or Ad-ZIP8 in the presence of rhodanine derivative or TPEN. The cellular localization of HIF-2 $\alpha$  was detected by immunofluorescence microscopy<sup>12,13,26</sup>. Cells cultured under the various conditions were fixed in 4% paraformaldehyde, permeabilized with 0.2% Triton X-100 in PBS, and serially blocked with Image-iT FX Signal Enhancer (Invitrogen) and PBS containing 1% bovine serum albumin. HIF-2 $\alpha$  and MTF1 were detected with primary antibodies against HIF-2 $\alpha$  (NB100-122; Novusbio, Centennial, CO) or MTF1 (NBP1-86380; Novusbio), followed by an Alexa Fluor 488-conjugated secondary antibody (Invitrogen). At least 200 cells were examined in multiple fields per condition, and the percentages of nuclear HIF-2 $\alpha$ - or MTF1-positive cells were quantified.

#### HIF-2 $\alpha$ and MTF1 reporter gene assays

The transcriptional activities of HIF-2 $\alpha$  and MTF1 in chondrocytes and FLS were determined as described previously<sup>12,13,26</sup>. The HIF-2 $\alpha$  promoter-reporter gene was constructed in a pGL3 vector by inserting four tandem repeats of the HIF-2 $\alpha$ -binding oligonucleotide into the upstream region of the SV40 promoter. Chondrocytes were transfected for 5 h with the HIF-2 $\alpha$  promoter-reporter gene (1  $\mu$ g) and a Renilla luciferase expression vector (0.1  $\mu$ g) using Lipofectamine 2000 (Invitrogen). Cells were harvested 24 h after treatment, and firefly and Renilla luciferase activities were measured using a Dual Luciferase Assay System (Promega, Madison, WI). The MTF1 reporter gene assay kit was obtained from SABiosciences (Solana Beach, CA). Chondrocytes were transfected for 5 h with a metal response element (MRE) reporter construct and a constitutive Renilla luciferase construct, using Lipofectamine 2000. The cells were harvested 24 h after treatment, and luciferase activity was measured. Transcriptional activity was normalized with Renilla luciferase activity, and the relative activity against vehicle-treated control group was presented.

#### Reverse transcription-polymerase chain reaction (RT-PCR) and quantitative PCR (qRT-PCR)

Total RNA extracted from mouse chondrocytes and FLS was reverse transcribed, and the resulting cDNA was amplified by PCR. The sequences of PCR primers are described previously<sup>11–14</sup>. qRT-PCR was performed in a CFX Connect Real-Time PCR Detection System (Bio-Rad, Hercules, CA) using SYBR Premix Ex Taq (TaKaRa Bio Inc., Shiga-ken, Japan). The relative amounts of each mRNA level were normalized to  $\beta$ -actin levels, and the differences in mRNA levels were calculated by the 2<sup>- $\Delta\Delta$ CT</sup> method<sup>27</sup>.

#### Western blot analysis

Total cell lysates were prepared using RIPA lysis buffer (150 mM NaCl, 1% NP-40, 50 mM Tris, 5 mM NaF), resolved by SDS-PAGE, and blotted to membranes, and cellular proteins were detected with appropriate antibodies (sc-13596 for HIF-2 $\alpha$  and sc-6216 for Lamin B; Santa Cruz Biotech, Dallas, TX). To detect secreted proteins, 900  $\mu$ L of serum-free conditioned medium was subjected to trichloroacetic acid precipitation, and the proteins were fractionated by SDS-PAGE, transferred to a nitrocellulose membrane, and detected using appropriate antibodies (ab52915 for MMP3 and ab51072 for MMP13; Abcam, Cambridge, UK).

#### Isothermal titration calorimetry (ITC)

The binding affinity of each rhodanine derivative to Zn<sup>2+</sup> ion was determined by isothermal titration calorimetry (ITC) using an Affinity ITC calorimeter (low-volume cell 190  $\mu$ L; TA Instruments, New Castle, DE) at 20°C<sup>28</sup>. Each rhodanine derivative was prepared in buffer containing 20 mM Tris-HCl, pH 7.5, and 150 mM NaCl. ZnCl<sub>2</sub> was loaded into a syringe (100  $\mu$ L of 0.1 mM solution). The desired rhodanine derivative (350  $\mu$ L of 0.05 mM) was placed in the cell of the calorimeter, and a titration curve was obtained by injecting 2- $\mu$ L aliquots of ZnCl<sub>2</sub> into the cell 25 times with an interval of 200 s between each injection. The enthalpy of the reaction ( $\Delta H^0$ ), the binding constant ( $K_d$ ), and the stoichiometry value ( $n$ ) were calculated from the heat changes ( $\delta H_i$ ) measured upon the association of the rhodanine derivative with Zn<sup>2+</sup> ion. The titration data were analyzed using the program NanoAnalyze (TA Instruments) and fitted into an independent binding model.

#### Statistical analysis

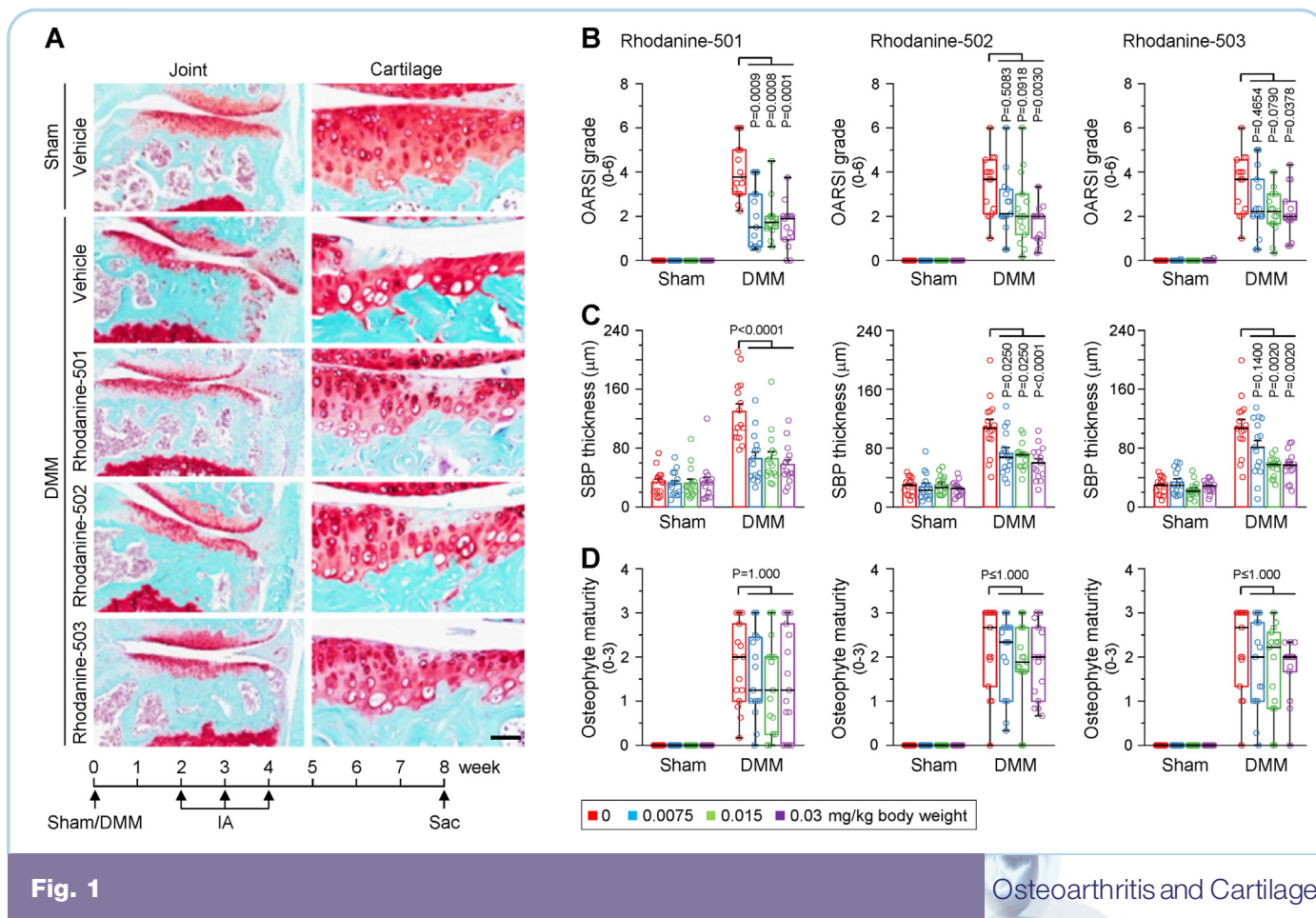
For statistical comparison of experimental groups, the data were analyzed by the Shapiro–Wilk test for normality and Levene's test for homogeneity of variance. Parametric data such as qRT-PCR, transcriptional activity, and Zn<sup>2+</sup> concentration were log-transformed before statistical analysis and compared by two-tailed paired *t*-test. Thickness of SBP was also log-transformed and compared by one-way analysis of variance (ANOVA) with Bonferroni's *post-hoc* test. Non-parametric data such as OARS grade, synovitis, and osteophyte maturity were compared using Kruskal–Wallis with Bonferroni's *post-hoc* test. Values for parametric data are shown as mean  $\pm$  s.e.m. with *P*-value, whereas values for non-parametric data are shown as median  $\pm$  interquartile range (IQR) with *P*-value. Details of statistical results such as 95% CI for difference between means or mean ranks are displayed in [Supplementary Table 1](#).

## Results

#### Rhodanine derivatives inhibit DMM-induced post-traumatic OA in mice

We first examined whether R-501 modulates post-traumatic OA in mice by IA injecting the derivative into DMM-operated mice at doses of 0.0075, 0.015, and 0.03 mg/kg body weight. We then extended our work to R-502 and R-503 at the same doses. These doses of the rhodanine derivatives did not cause any abnormality in joint tissue histology or morphology [Fig. 1(A)]. OA manifestations were examined at 8 weeks after DMM surgery. IA injection of each rhodanine derivative significantly inhibited DMM-induced cartilage destruction [Fig. 1(A) and (B)]. The rhodanine derivatives also inhibited SBP thickening [Fig. 1(A) and (C)], suggesting that they decreased subchondral bone sclerosis. In contrast to these findings,





**Rhodanine derivatives inhibit DMM-induced post-traumatic OA in mice.** Sham- and DMM-operated mice were IA injected with the indicated concentrations of rhodanine derivatives and sacrificed at 8 weeks after DMM surgery ( $n = 15$  mice per group). (A) Representative safranin-O staining images of joint sections from sham- and DMM-operated mice that were IA injected with vehicle or 0.03 mg/kg body weight of the indicated rhodanine derivative. (B–D) Quantitation of OARS grade (B), subchondral bone plate (SBP) thickness (C), and osteophyte maturity (D). Data for OARS grade and osteophyte maturity are presented as median  $\pm$  interquartile range (IQR). The significance was evaluated by Kruskal–Wallis with *post-hoc* Bonferroni test. Values for SBP thickness represent the mean  $\pm$  S.E.M., and significance was evaluated by one-way ANOVA with *post-hoc* Bonferroni test. Scale bars: 50  $\mu$ m.

DMM-induced osteophyte maturity was not significantly modulated by the rhodanine derivatives in our experimental system [Fig. 1(A) and (D)]. Statistical details such as 95% CI of the difference between the means and mean rank were presented in [Supplementary Table 1](#). Our results collectively suggest that the tested rhodanine derivatives reduce DMM-induced OA cartilage destruction and subchondral bone sclerosis in mice.

#### Rhodanine derivatives inhibit HIF-2 $\alpha$ -induced OA pathogenesis in mice

Next, we examined the effects of the rhodanine derivatives on HIF-2 $\alpha$ -induced OA development. We previously demonstrated that adenoviral overexpression of HIF-2 $\alpha$  in whole-joint tissues is sufficient to cause OA pathogenesis<sup>11,12</sup>. Consistently, we herein observed ECM loss (assessed by modified Mankin's score) and synovitis at week 3 after the first IA injection of Ad-HIF-2 $\alpha$  [Fig. 2(A) and (B)], whereas cartilage destruction (OARS grade), SBP thickening, and osteophyte formation were observed at 8 weeks after

the first IA injection [Fig. 2(C) and (D)]. IA injection of each rhodanine derivative significantly inhibited all tested manifestations of HIF-2 $\alpha$ -induced OA, including synovitis, cartilage ECM loss, cartilage destruction, SBP thickening, and osteophyte formation [Fig. 2(A)–2(D)]. Details of statistical results are presented in [Supplementary Table 1](#).

To begin elucidating the mechanisms through which these rhodanine derivatives inhibit OA pathogenesis, we examined their effects on the nuclear localization and transcriptional activity of HIF-2 $\alpha$  in chondrocytes. Immunofluorescence microscopy revealed that Ad-HIF-2 $\alpha$ -infected chondrocytes exhibited nuclear localization of HIF-2 $\alpha$  and a significant increase of HIF-2 $\alpha$  transcriptional activity [Fig. 3(A)–(C)]. Each rhodanine derivative significantly inhibited this nuclear localization and transcriptional activation of HIF-2 $\alpha$  [[Supplementary Table 1](#)], but did not alter the mRNA or protein levels of HIF-2 $\alpha$  [Fig. 3(D)]. Therefore, rhodanine derivatives appear to inhibit HIF-2 $\alpha$ -induced OA by inhibiting the nuclear translocation of HIF-2 $\alpha$  and thereby blocking its transcriptional activity.

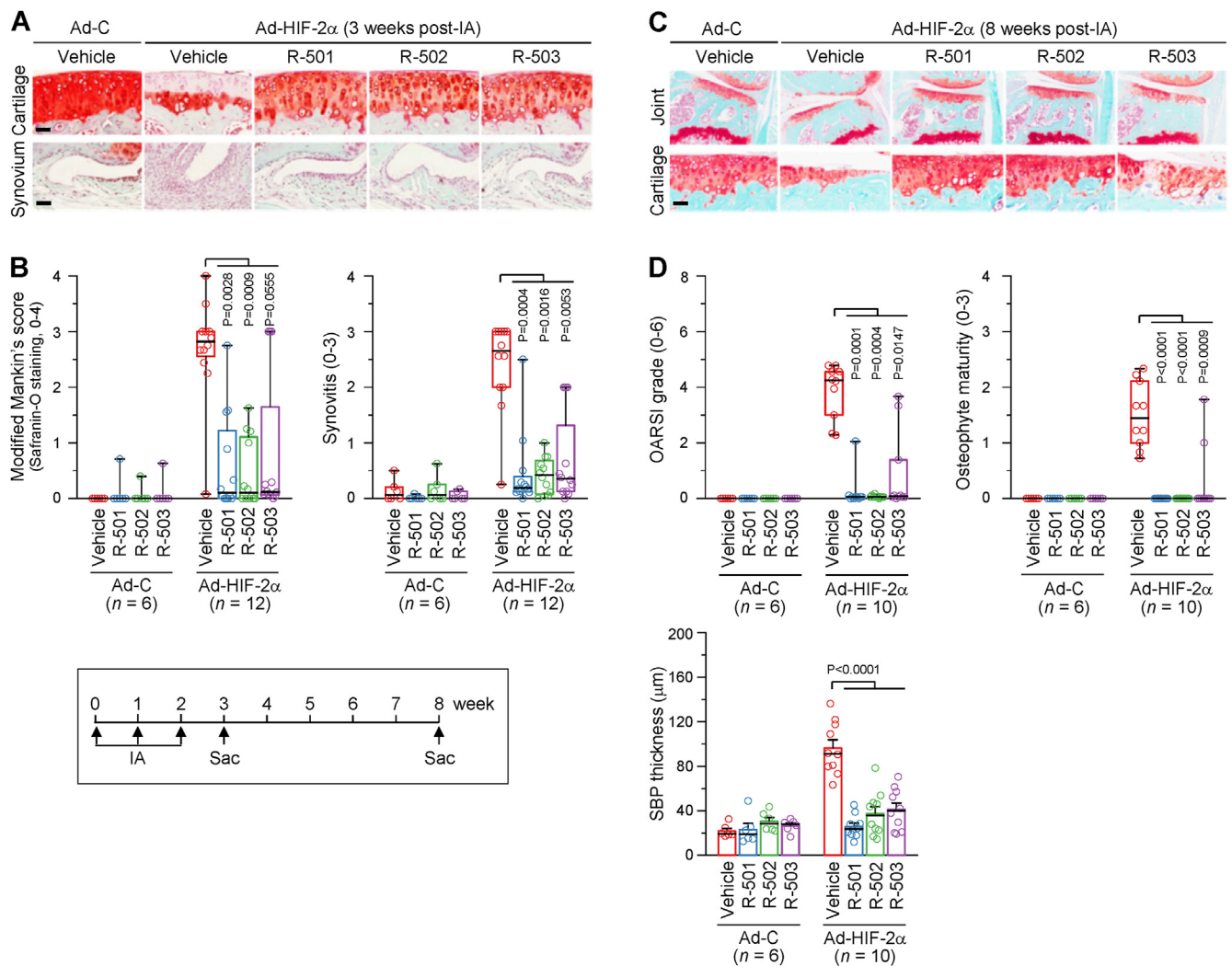


Fig. 2

Osteoarthritis and Cartilage

**Rhodanine derivatives inhibit HIF-2 $\alpha$ -induced OA pathogenesis in mice.** Mice were IA injected with  $1 \times 10^9$  PFU of Ad-C or Ad-HIF-2 $\alpha$  plus the indicated rhodanine (R) derivative (0.03 mg/kg body weight) once weekly for 3 weeks. Mice were sacrificed at 3 weeks (A and B) or 8 weeks (C and D) after the first IA injection. Presented are representative safranin-O and hematoxylin staining images of joint sections (A and C) and quantitation of OA manifestations (B and D). Data for Mankin's score, synovitis, OARSIS grade, and osteophyte maturity are plotted as median  $\pm$  interquartile range (IQR), and significance was evaluated by Kruskal–Wallis with *post-hoc* Bonferroni test. Values for SBP thickness are presented as mean  $\pm$  S.E.M. and significance was evaluated by one-way ANOVA with *post-hoc* Bonferroni test. Scale bars: 50  $\mu$ m.

#### Rhodanine derivatives inhibit ZIP8-induced OA pathogenesis in mice

We previously showed that adenoviral overexpression of ZIP8 in joint tissues causes OA pathogenesis<sup>13,14</sup>. ZIP8 overexpression in chondrocytes causes an influx of Zn<sup>2+</sup>, activation of the metal-dependent transcription factor MTF1, and expression of matrix-degrading enzymes, and thereby triggers OA pathogenesis in mice<sup>13,14</sup>. Consistent with our previously reported results<sup>13</sup>, cartilage ECM loss and synovial inflammation were observed at 3 weeks after IA injection of Ad-ZIP8 in the present work [Fig. 4(A) and (B)]. These OA manifestations were significantly reduced by the co-injection of each rhodanine derivative [Fig. 4(A) and (B); Supplementary Fig. 3]. Cartilage destruction, SBP thickening, and

osteophyte formation were observed at 8 weeks after the first IA injection, and all of these OA manifestations were almost completely inhibited by IA administration of each rhodanine derivative [Fig. 4(C) and (D); Supplementary Fig. 4; Supplementary Table 1].

The mechanisms through which the rhodanine derivatives inhibited ZIP8-induced OA pathogenesis were elucidated by exploring how they affect Zn<sup>2+</sup> homeostasis and downstream regulatory pathways. The increase seen in the cellular Zn<sup>2+</sup> levels of chondrocytes treated with IL-1 $\beta$  [Fig. 5(A) and (B)] or infected with Ad-ZIP8 [Fig. 5(C) and (D)] were not markedly modulated by the examined rhodanine derivatives, whereas the metal ion chelator, TPEN [N, N, N', N'-tetrakis(2-pyridinylmethyl)-1,2-ethanediamine],

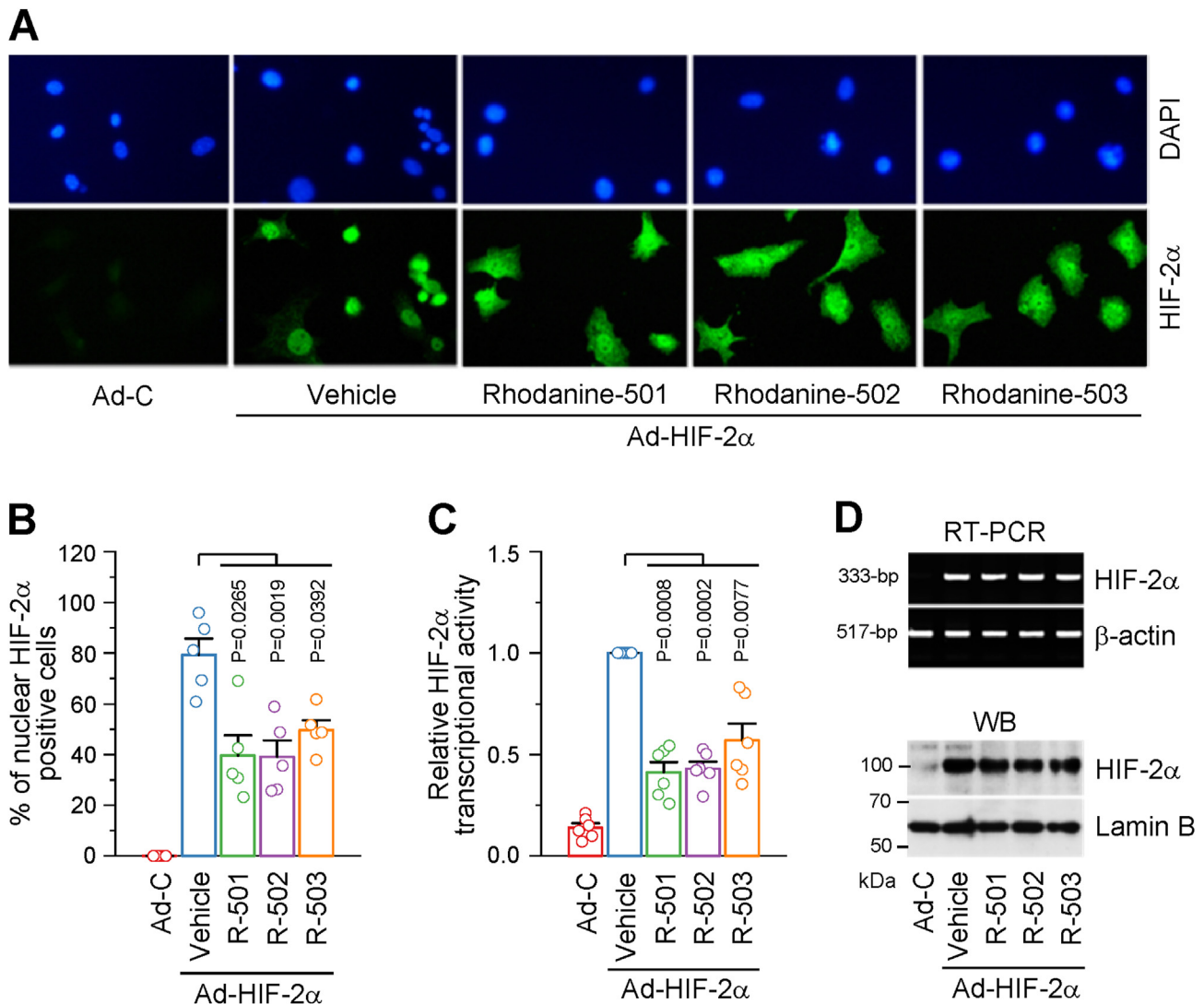


Fig. 3

**Rhodanine derivatives inhibit the transcriptional activity of HIF-2α in chondrocytes.** Primary-culture mouse chondrocytes were infected with 800 MOI of Ad-C or Ad-HIF-2α and treated with 1 μM of the indicated rhodanine (R) derivative for 24 h ( $n \geq 5$  independent experiments). Representative immunofluorescence microscopic images of DAPI and HIF-2α (A), quantitation of nuclear HIF-2α-positive chondrocytes (B), relative HIF-2α transcriptional activity (C), and representative RT-PCR and Western blot images of HIF-2α (D) are shown. Means  $\pm$  s.e.m. were assessed by paired *t*-test (B and C).

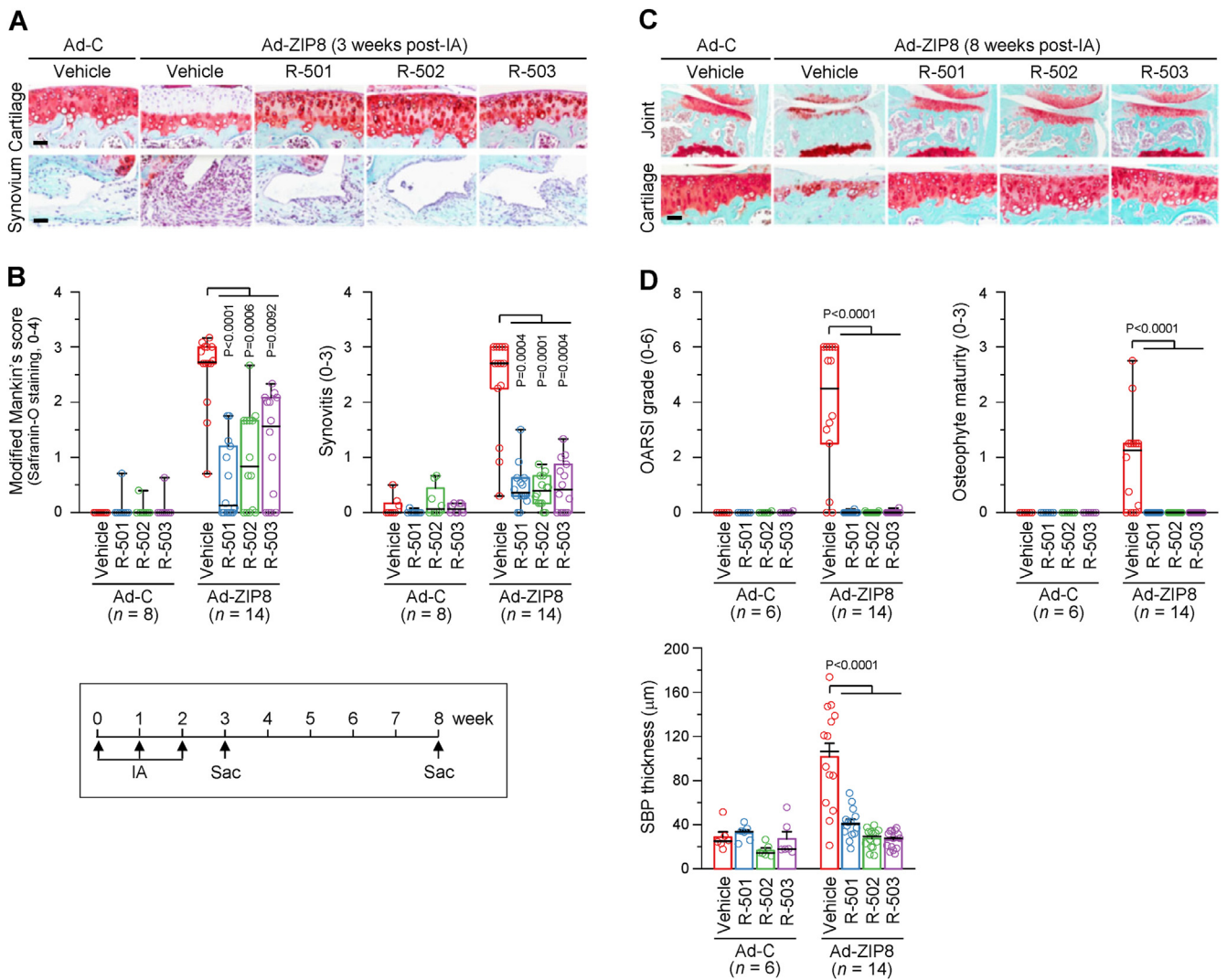
significantly reduced the cellular Zn<sup>2+</sup> levels [Fig. 5(A)–(D); Supplementary Table 1]. This suggests that rhodanine derivatives do not modulate the ZIP8-mediated Zn<sup>2+</sup> influx in chondrocytes. However, the activation of the Zn<sup>2+</sup>-dependent transcription factor, MTF1, by IL-1β treatment or ZIP8 overexpression was significantly inhibited by the rhodanine derivatives [Fig. 6(A); Supplementary Table 1]. Our isothermal titration calorimetry assay revealed that the rhodanine derivatives did not exhibit significant binding affinity for Zn<sup>2+</sup> ion [Fig. 6(B)]. However, the nuclear localization of MTF1 in chondrocytes treated with IL-1β or Ad-ZIP8 was markedly inhibited by the rhodanine derivatives or TPEN [Fig. 6(C) and (D)]. Our results indicate that the rhodanine derivatives do not directly bind to Zn<sup>2+</sup>, but rather inhibit the nuclear translocation and

consequent transcriptional activation of MTF1 to inhibit ZIP8-mediated OA pathogenesis.

*Rhodanine derivatives inhibit the expression of matrix-degrading enzymes in chondrocytes*

As OA cartilage destruction is primarily caused by the upregulation of matrix-degrading enzymes<sup>5,6</sup>, we examined how the rhodanine derivatives affect the expression levels of MMP3, MMP13, and ADAMTS5, which are known to play important roles in animal models of OA<sup>7–9</sup>. The IL-1β-induced upregulations of the encoding MMP3, MMP13, and ADAMTS5 were significantly inhibited by R-501 and R-502, whereas R-503 exhibited less or no





significant inhibitory effect [Fig. 7(A); Supplementary Fig. 5(A); Supplementary Table 1]. Similarly, the upregulations of these mRNAs in chondrocytes overexpressing HIF-2 $\alpha$  or ZIP8 [Fig. 7(B) and (C); Supplementary Fig. 5(B) and 5(C)] were also significantly inhibited by the rhodanine derivatives [Supplementary Table 1]. Consistently, the levels of MMP3 and MMP13 secreted by chondrocytes treated with IL-1 $\beta$ , Ad-HIF-2 $\alpha$ , or Ad-ZIP8 were also markedly reduced by the rhodanine derivatives [Fig. 7(D)]. Our results indicate that the rhodanine derivative-mediated down-regulation of matrix-degrading enzymes appears to be at least one mechanism through which the rhodanine derivatives inhibit OA cartilage destruction.

#### Rhodanine derivatives modulate the functions of FLS

Multiple cell types of joint tissues are involved in the OA process. We therefore examined whether the rhodanine derivatives could modulate HIF-2 $\alpha$  signaling and the zinc-ZIP8-MTF1 axis in mouse FLS. Overexpressed HIF-2 $\alpha$  was localized in the nuclei of FLS and exhibited increased transcriptional activity [Supplementary Fig. 6(A)–6(C)], which was significantly inhibited by each of the rhodanine derivatives [Supplementary Fig. 6(B) and (C); Supplementary Table 1]. However, the mRNA and protein expression levels of HIF-2 $\alpha$  remained unaltered [Supplementary Fig. 6(D)]. Regarding the zinc-ZIP8-MTF1 axis in FLS, we found that ZIP8

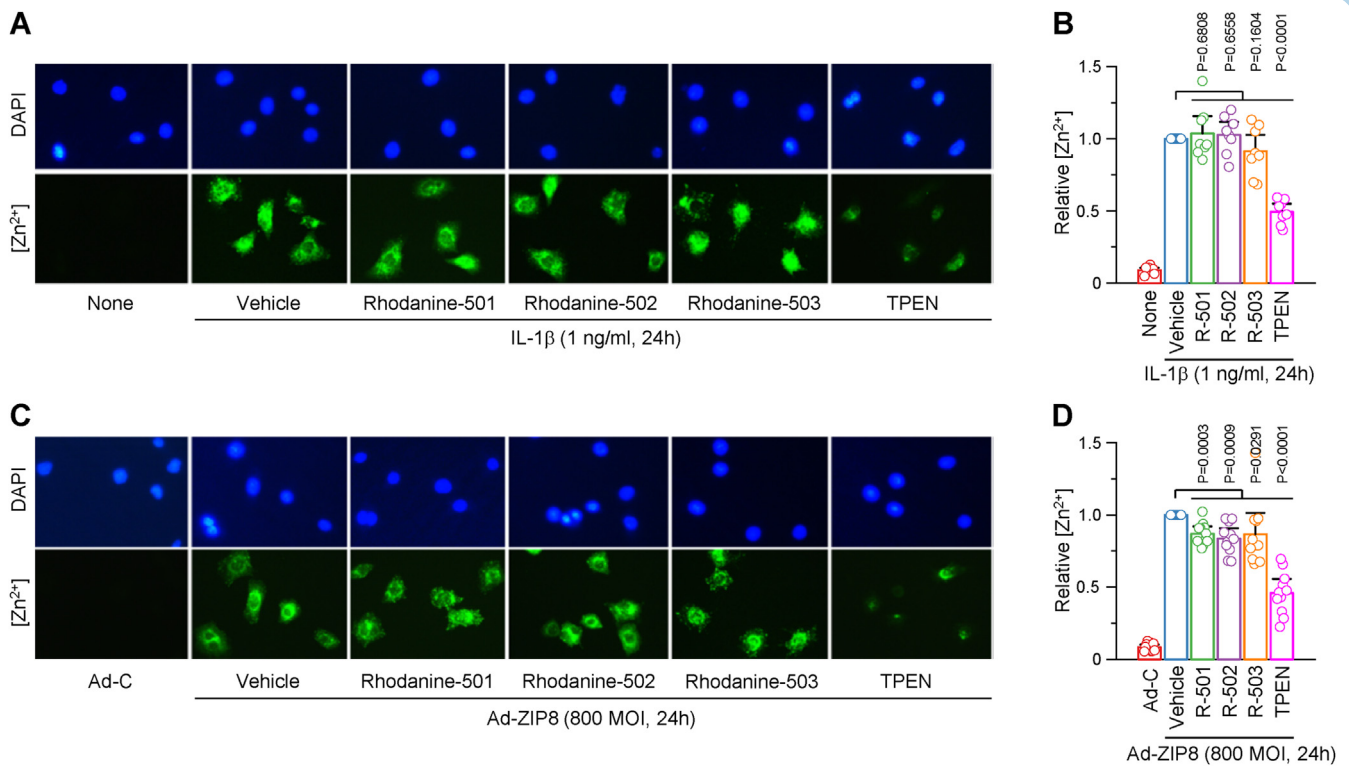


Fig. 5

Osteoarthritis and Cartilage

**Rhodanine derivatives do not modulate zinc homeostasis in chondrocytes.** (A and B) Primary-culture mouse chondrocytes were treated with IL-1 $\beta$  in the absence or presence of 1  $\mu$ M of the indicated rhodanine derivative for 24 h. The metal ion chelator, TPEN (1  $\mu$ M), was used as a positive control. Representative fluorescence microscopic images of DAPI and Zn<sup>2+</sup> (A) and quantitation of relative Zn<sup>2+</sup> concentrations (B,  $n = 8$  independent experiments). (C and D) Mouse chondrocytes were infected with Ad-ZIP8 in the absence or presence 1  $\mu$ M of the indicated rhodanine derivative or TPEN for 24 h. Representative fluorescence microscopic images of DAPI and Zn<sup>2+</sup> (C) and quantitation of relative zinc ion concentrations (D,  $n = 11$  independent experiments). Values are presented as the mean  $\pm$  S.E.M. Significance was evaluated by paired  $t$ -test.

overexpression or IL-1 $\beta$  treatment increased the cellular zinc level in FLS. The rhodanine derivatives did not modulate the ZIP8-mediated influx of Zn<sup>2+</sup> into FLS [Supplementary Fig. 7(A)–(D)]. However, the nuclear localization of the MTF1 was significantly inhibited by the rhodanine derivatives, as was the transcriptional activation of MTF1 [Supplementary Fig. 7(E)–(I); Supplementary Table 1]. These results indicate that the rhodanine derivatives inhibit MTF1 transcriptional activity by blocking its nuclear translocation.

Finally, we explored the effects of the rhodanine derivatives on the expression levels of MMP3, MMP13, and ADAMTS5 in FLS. The encoding mRNAs were found to be upregulated in FLS under treatment with IL-1 $\beta$  or overexpression of HIF-2 $\alpha$  or ZIP8, and the rhodanine derivatives significantly inhibited the upregulations of these enzymes at the mRNA and protein levels [Supplementary Fig. 8(A)–(D); Supplementary Table 1]. Our results collectively indicate that the tested rhodanine derivatives inhibit HIF-2 $\alpha$  signaling and the zinc-ZIP8-MTF1 axis and thereby downregulate the expression levels of matrix-degrading enzymes in both chondrocytes and synoviocytes, suggesting that both cell types are involved in the inhibitory effects of these rhodanine derivatives on OA pathogenesis [Fig. 7(E)].

## Discussion

Although OA is a major cause of disability worldwide, there is currently no approved disease-modifying OA drug (DMOAD)<sup>29</sup>. We herein reveal that rhodanine derivatives could be novel DMOADs, as the IA administration of three tested rhodanine derivatives significantly reduced OA pathogenesis in various mouse models. The tested rhodanine derivatives exhibited therapeutic potential against not only DMM-induced post-traumatic OA but also against the OA pathogenesis caused by the adenoviral overexpression of HIF-2 $\alpha$  or ZIP8. We previously demonstrated that the chondrocyte-specific overexpression of HIF-2 $\alpha$  or ZIP8 or their adenoviral overexpression in whole-joint tissues causes OA development, whereas deficiency of the genes encoding HIF-2 $\alpha$  or ZIP8 was found to be sufficient to reduce DMM-induced post-traumatic OA in mice<sup>11–14</sup>. Based on our current observations, we hypothesized that these rhodanine derivatives would decrease DMM-induced OA through the inhibition of the HIF-2 $\alpha$  and/or ZIP8 signaling pathways. Indeed, we observed that the selected rhodanine derivatives inhibited the transcriptional activity of HIF-2 $\alpha$  and Zn<sup>2+</sup>-dependent MTF1 in chondrocytes and synoviocytes by blocking the nuclear localizations of these transcription factors. Additionally, the rhodanine derivative-mediated inhibition of the HIF-2 $\alpha$ - or ZIP8-



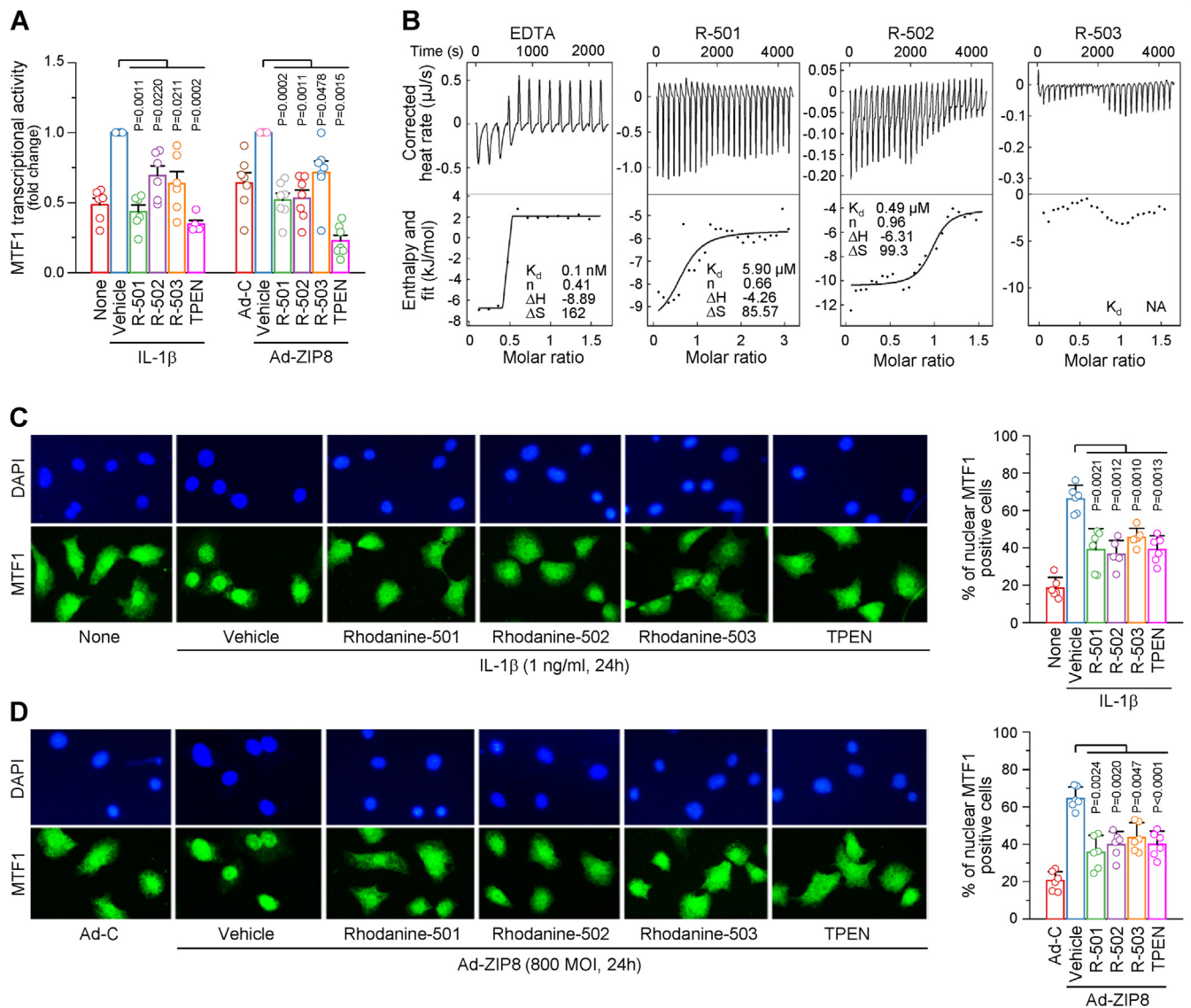


Fig. 6

Osteoarthritis and Cartilage

**Rhodanine derivatives inhibit MTF1 transcriptional activity without binding to zinc ion in chondrocytes.** (A) Relative transcriptional activity of MTF1 in mouse chondrocytes treated with IL-1 $\beta$  (1 ng/mL) or infected with 800 MOI of Ad-C or Ad-ZIP8 in the absence or presence of 1  $\mu$ M of the indicated rhodanine derivative for 24 h ( $n = 6$  independent experiments). TPEN (1  $\mu$ M) was used as a positive control. (B) Isothermal titration calorimetry (ITC) was used to measure the binding affinity of rhodanine derivatives for Zn $^{2+}$ . Each rhodanine derivative was dissolved at 0.05 mM in 10% DMSO and titrated with 0.1 mM of ZnCl $_2$ . EDTA was used as a positive control for the binding to Zn $^{2+}$ . The  $K_d$  of EDTA was the lowest value measurable by the ITC experiment. Presented are representative results of six independent experiments. (C and D) Chondrocytes were treated with IL-1 $\beta$  (C) or infected with 800 MOI of Ad-C or Ad-ZIP8 (D) in the absence or presence of 1  $\mu$ M of the indicated rhodanine derivative or TPEN. Representative immunostaining images of DAPI and MTF1 (left panels) and quantitation of nuclear MTF1-positive chondrocytes (right panels,  $n = 6$  independent experiments). Values are presented as mean  $\pm$  s.e.m. and were assessed by paired  $t$ -test (A, C, and D).

induced upregulations of matrix-degrading enzymes appears to be responsible for the ability of these compounds to inhibit OA cartilage destruction. The ability of the tested rhodanine derivatives to inhibit OA cartilage destruction, which is a hallmark of OA, strongly suggests that these rhodanine derivatives could be considered novel DMOADs.

Currently, various novel chemicals have been suggested as potential DMOADs. For instance, GLPG1972/S201086 and UBX0101,

which target ADAMTS5 and p53/MDM2, respectively, exhibited therapeutic potential in an animal model of OA and have been investigated in phase two clinical studies in patients with knee OA<sup>30,31</sup>. Specific chemical inhibitors targeting OA-regulating proteins in cartilage have also been investigated as potential DMOADs, including inhibitor of secretory phospholipase A2, bromodomain-containing-protein-4, and cyclin-dependent-kinase-9<sup>32,33</sup>. Some drugs approved by the U.S. Food and Drug Administration for other

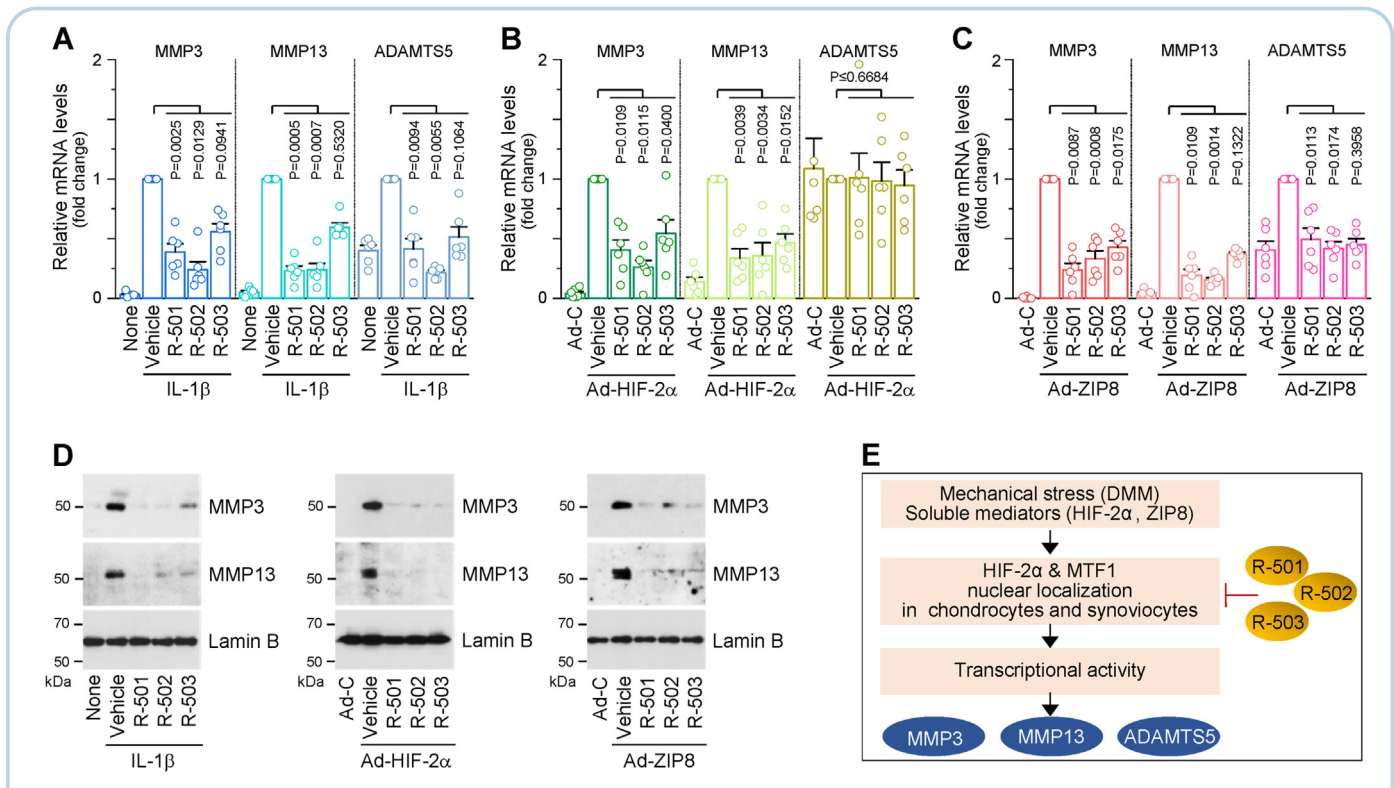


Fig. 7

Osteoarthritis and Cartilage

**Rhodanine derivatives inhibit the expression of matrix-degrading enzymes in chondrocytes.** (A–D) Mouse chondrocytes were treated with IL-1 $\beta$  (1 ng/mL) or infected with 800 MOI of Ad-C, Ad-HIF-2 $\alpha$ , or Ad-ZIP8 for 6 h in the absence and presence of 2  $\mu$ M of the indicated rhodanine derivative ( $n = 6$  independent experiments). mRNA levels of MMP3, MMP13, and ADAMTS5 were quantified by qRT-PCR analysis (A–C). Protein levels of secreted extracellular MMP3 and MMP13 were determined by Western blot analysis (D). (E) Schematic illustration for the action of rhodanine derivatives on experimental OA pathogenesis. Values are presented as means  $\pm$  s.e.m., and were assessed by paired  $t$ -test.

diseases are known to target proteins that regulate OA pathogenesis, and thus may be investigated for their potential to be repurposed as DMOADs. For example, the antidepressant, paroxetine, which targets G protein-coupled receptor kinase 2, has shown potential as a DMOAD in animal model-based studies<sup>34</sup>. Tofacitinib, which inhibits Janus kinase and is used to treat rheumatoid arthritis, psoriatic arthritis, and inflammatory bowel disease, was found to significantly lower the arthritis score in a rat OA model upon IA administration<sup>35</sup>.

In addition to the above DMOAD candidates, our current results suggest that all three examined rhodanine derivatives could be potential DMOADs. We analyzed several pharmacokinetic parameters of R-501 in rats and mice (manuscript in preparation). In rats, we found that the bioavailability of orally administered R-501 is 36%. In mice, we found that the plasma concentration of R-501 peaked at 2 h after administration and the half-life of R-501 is 3.88 h in plasma (manuscript in preparation). In the present study, we employed IA injection of rhodanine derivatives at dosages of 0.0075, 0.015, and 0.03 mg/kg body weight. At these dosages, we did not see any morphological or histological abnormality in derivative-treated joint tissues. Although these observations indicate that the tested rhodanine derivatives do not exert apparent toxicity, future work should examine the possible side effects of long-term rhodanine derivative exposure in mice and rats.

The clinical management of OA with potential DMOADs has been complicated by the lack of an effective drug-delivery system<sup>36</sup>. Many of these therapeutics target chondrocytes embedded in the cartilage ECM, which poses significant delivery challenges for many promising drugs<sup>37,38</sup>. Recently, nanoparticle-based targeted drug delivery has been exploited in the treatment of OA<sup>32,37</sup>. However, the delivery efficiency of rhodanine derivatives to chondrocytes of cartilage has not yet been determined. Moreover, rhodanine derivatives may modulate other cell types of joint tissues, such as synoviocytes, to inhibit OA pathogenesis. Indeed, we demonstrated that rhodanine derivatives inhibit HIF-2 $\alpha$  and the zinc-ZIP8-MTF1 axis in both chondrocytes and synoviocytes, suggesting that both cell types contribute to the ability of the rhodanine derivatives to inhibit OA pathogenesis. Therefore, it is likely that rhodanine derivatives dysregulate the cytoplasm-to-nucleus transport of HIF-2 $\alpha$  and MTF1. We cannot at this point speak to the human relevance of rhodanine derivatives as possible OA therapeutics. As we examined the therapeutic potential of the rhodanine derivatives strictly in mouse models of experimental OA, confirmatory and mechanistic studies in human chondrocytes and synoviocytes will be needed to support the human translation of this work.

In conclusion, we found that IA administration of three rhodanine derivatives significantly reduced OA pathogenesis in

various mouse models, demonstrating the disease-modifying therapeutic potential of these rhodanine derivatives against OA pathogenesis.

#### Author contributions

YL and JSK: study design, data acquisition, data analysis and interpretation, manuscript preparation and approval; JY, SKK, YS, HJK, JHC: data acquisition and manuscript approval; YJI: study design and analysis of ITC and manuscript approval; MJK, KLY, and JCY: preparation of rhodanine derivatives and manuscript preparation and approval; JSC: funding acquisition, study design, data interpretation, manuscript preparation and approval. JSC ([jschun@gist.ac.kr](mailto:jschun@gist.ac.kr)) takes responsibility for the integrity of this work.

#### Conflict of interest

The authors declare that they have no conflicts of interest.

#### Role of the funding source

The funding source had no role in the study design, collection, analysis and interpretation of data, nor in the writing of the manuscript and decision to submit for publication.

#### Acknowledgements

This work was supported by grants from the National Research Foundation of Korea (2016R1A3B1906090 and 2016R1A5A1007318) and the Korea Health Industry Development Institute (H114C3484).

#### Supplementary data

Supplementary data to this article can be found online at <https://doi.org/10.1016/j.joca.2022.04.005>.

#### References

- Punzi L, Galozzi P, Luisetto R, Favero M, Ramonda R, Oliviero F, et al. Post-traumatic osteoarthritis: overview on pathogenic mechanisms and role of inflammation. *RMD Open* 2016;2:e000279.
- Berenbaum F, Griffin TM, Liu-Bryan R. Metabolic regulation of inflammation in osteoarthritis. *Arthritis Rheum* 2017;69:9–21.
- Loeser RF, Collins JA, Diekmann BO. Ageing and the pathogenesis of osteoarthritis. *Nat Rev Rheumatol* 2016;12:412–20.
- Martel-Pelletier J, Barr AJ, Cicuttini FM, Conaghan G, Cooper C, Goldring MB, et al. Osteoarthritis. *Nat Rev Dis Prim* 2016;2:16072.
- Oikonomopoulou K, Diamandis EP, Hollenberg MD, Chandran V. Proteinases and their receptors in inflammatory arthritis: an overview. *Nat Rev Rheumatol* 2018;14:170–80.
- Mehana ESE, Khafaga AF, El-Blehi SS. The role of matrix metalloproteinases in osteoarthritis pathogenesis: an updated review. *Life Sci* 2019;234:116786.
- Blom AB, van Lent PL, Libregts S, Holthuysen AE, van der Kraan PM, van Rooijen N, et al. Crucial role of macrophages in matrix metalloproteinase-mediated cartilage destruction during experimental osteoarthritis: involvement of matrix metalloproteinase 3. *Arthritis Rheum* 2007;56:147–57.
- Little CB, Barai A, Burkhardt D, Smith SM, Fosang AJ, Werb Z, et al. Matrix metalloproteinase 13-deficient mice are resistant to osteoarthritic cartilage erosion but not chondrocyte hypertrophy or osteophyte development. *Arthritis Rheum* 2009;60:3723–33.
- Glasson SS, Askew R, Sheppard B, Carito B, Blanchet T, Ma HL, et al. Deletion of active ADAMTS5 prevents cartilage degradation in a murine model of osteoarthritis. *Nature* 2005;434:644–7.
- Glasson SS, Blanchet TJ, Morris EA. The surgical destabilization of the medial meniscus (DMM) model of osteoarthritis in the 129/SvEv mouse. *Osteoarthritis Cartilage* 2007;15:1061–9.
- Yang S, Kim J, Ryu JH, Oh H, Chun CH, Kim BJ, et al. Hypoxia-inducible factor-2 $\alpha$  is a catabolic regulator of osteoarthritic cartilage destruction. *Nat Med* 2010;16:687–93.
- Yang S, Ryu JH, Oh H, Jeon J, Kwak JS, Kim JH, et al. NAMPT (visfatin), a direct target of hypoxia-inducible factor-2 $\alpha$ , is an essential catabolic regulator of osteoarthritis. *Ann Rheum Dis* 2015;74:595–602.
- Kim JH, Jeon J, Shin M, Won Y, Lee M, Lee G, et al. Regulation of the catabolic cascade in osteoarthritis by the zinc-ZIP8-MTF1 axis. *Cell* 2014;156:730–43.
- Won Y, Shin Y, Chun CH, Cho Y, Ha CW, Kim JH, et al. Pleiotropic roles of metallothioneins as regulators of chondrocyte apoptosis and catabolic and anabolic pathways during osteoarthritis pathogenesis. *Ann Rheum Dis* 2016;75:2045–52.
- Kaminsky D, Kryshchshyn A, Lesyk R. Recent developments with rhodanine as a scaffold for drug discovery. *Expert Opin Drug Discov* 2017;1388370.
- You JC, Han GH, Lee CH, Song DN, Chun KH. Rhodanine Derivatives, Methods for Preparing Same, and Pharmaceutical Composition for the Prevention or Treatment of AIDS Containing the Rhodanine Derivatives as Active Ingredients 2014. US patent 8,759,536 B2.
- Kim MJ, Kim SH, Park JA, Yu KL, Kim BS, Lee ES, et al. Identification and characterization of a new type of inhibitor against the human immunodeficiency virus typ-1 nucleocapsid protein. *Retrovirology* 2015;12:90.
- Incerti M, Crasci L, Vicini P, Aki P, Yalcin I, Ertan-Bolelli T, et al. 4-thiazolidinone derivatives as MMP inhibitors in tissue damage: synthesis, biological evaluation and docking studies. *Molecules* 2018;23:415.
- Panico AM, Vicini P, Geronikaki A, Incerti M, Cardile V, Crasci L, et al. Heteroarylmino-4-thiazolidinones as inhibitors of cartilage degradation. *Bioorg Chem* 2011;39:48–52.
- Choi WS, Lee G, Song WH, Koh JT, Yang J, Kwak JS, et al. The CH25H-CYP7B1-ROR $\alpha$  axis of cholesterol metabolism regulates osteoarthritis. *Nature* 2019;566:254–8.
- Arifin WN, Zahiruddin WM. Sample size calculation in animal studies using resource equation approach. *Malays J Med Sci* 2017;24:101–5.
- Glasson SS, Chambers MG, Van den Berg WB, Little CB. The OARSI histopathology initiative - recommendations for histological assessments of osteoarthritis in the mouse. *Osteoarthritis Cartilage* 2010;18:S17–23.
- Mainil-Varlet P, Schiavinato A, Ganster MM. Efficacy evaluation of a new hyaluronan derivative HYADD 4-G to maintain cartilage integrity in a rabbit model of osteoarthritis. *Cartilage* 2013;4:28–41.
- Krenn V, Morawietz L, Burmester GR, Kinne RW, Mueller-Ladner U, Muller B, et al. Synovitis score: discrimination between chronic low-grade and high-grade synovitis. *Histopathology* 2006;49:358–64.
- Gosset M, Berenbaum F, Thirion S, Jacques C. Primary culture and phenotyping of murine chondrocytes. *Nat Protoc* 2008;3:1253–60.



26. Oh H, Kwak JS, Yang S, Gong MK, Kim JH, Rhee J, *et al.* Reciprocal regulation by hypoxia-inducible factor-2 $\alpha$  and the NAMPT-NAD<sup>+</sup>-SIRT axis in articular chondrocytes is involved in osteoarthritis. *Osteoarthritis Cartilage* 2015;23:2288–96.
27. Livak Kenneth J, Schmittgen Thomas D. Analysis of relative gene expression data using real-time quantitative PCR and the 2<sup>- $\Delta\Delta$ CT</sup> method. *Methods* 2001;25:402–8.
28. Tong J, Tan L, Chun CJ, Im YJ. Structural basis of human ORP1-Rab7 interaction for the late-endosome and lysosome targeting. *PLoS One* 2019;14, e0211724.
29. Hunter DJ, Schofield D, Callander E. The individual and socio-economic impact of osteoarthritis. *Nat Rev Rheumatol* 2014;17:437–41.
30. Brebion F, Gosmini R, Deprez P, Varin M, Peixo C, Alvey L, *et al.* Discovery of GLPG1972/S201086, a potent, selective, and orally bioavailable ADAMTS-5 inhibitor for the treatment of osteoarthritis. *J Med Chem* 2021;64:2937–52.
31. Jeon OH, Kim C, Laberge RM, Demaria M, Rathod S, Vasserot AP, *et al.* Local clearance of senescent cells attenuates the development of post-traumatic osteoarthritis and creates a pro-regenerative environment. *Nat Med* 2017;23:775–81.
32. Wei Y, Yan L, Luo L, Gui T, Jang B, Amirshaghghi A, *et al.* Phospholipase A2 inhibitor-loaded micellar nanoparticles attenuate inflammation and mitigate osteoarthritis progression. *Sci Adv* 2021;7, eabe6374.
33. Fukui T, Yik JHN, Doyran B, Davis J, Haudenschild AK, Adamopoulos IE, *et al.* Bromodomain-containing-protein-4 and cyclin-dependent-kinase-9 inhibitors interact synergistically in vitro and combined treatment reduces post-traumatic osteoarthritis severity in mice. *Osteoarthritis Cartilage* 2021;29:68–77.
34. Carlson EL, Karuppagounder V, Pinamont WJ, Yoshioka NK, Ahmad A, Schott EM, *et al.* Paroxetine-mediated GRK2 inhibition is a disease-modifying treatment for osteoarthritis. *Sci Transl Med* 2021;13, eaau8491.
35. Chiu YS, Bamodu QA, Fong IH, Lee WH, Lin CC, Lu CH, *et al.* The JAK inhibitor Tofacitinib inhibits structural damage in osteoarthritis by modulating JAK1/TNF-alpha/IL-6 signaling through Mir-149-5p. *Bone* 2021;151:116024.
36. Didomenico CD, Lintz M, Bonassar LJ. Molecular transport in articular cartilage-what have we learned from the past 50 years? *Nat Rev Rheumatol* 2018;14:393–403.
37. Kumar S, Adjei IM, Brown SB, Liseth O, Sharma B. Manganese dioxide nanoparticles protect cartilage from inflammation-induced oxidative stress. *Biomaterials* 2019: 119467.
38. Geiger BC, Wang S, Fadera Jr RF, Grodzinsky AJ, Hammond RT. Cartilage-penetrating nanocarriers improve delivery and efficacy of growth factor treatment of osteoarthritis. *Sci Transl Med* 2018;10:eaat8800.